Supporting information for: Large Area, Soft Crystalline Thin Films of N,N',N''-trialkyltriazatriangulenium Salts with Homeotropic Alignement of the Discotic Cores in a Smectic Matrix.

Large Area, Soft Crystalline Thin Films of *N,N',N''*-trialkyltriazatriangulenium Salts with Homeotropic Alignment of the Discotic Cores in a Smectic Lattice.

By *Thomas J. Sørensen, Christoffer B. Hildebrandt, Jonas Elm, Jens W. Andreasen, Anders Ø. Madsen, Fredrik Westerlund* and *Bo W. Laursen**

Table of Contents

Synthesis of N,N',N''-tris(3-methylpentyl)triazatriangulenium·BF_4 and dioctyl-diazaoxatriangulenium·BF_4

Sythesis of (3-methylpentyl)$_3$-TATA$^+$:

(DMP)$_3$C$^+$ tetra fluoroborate (306 mg, 1.01 mmol) was dissolved in 3.0 ml NMP and *rac*-3-methylpentylamine (4.8 ml , 35.4 mmol) was added to the solution. The reaction mixture was refluxed with free access to the atmosphere for 23 hours, and after cooling to room temperature diethyl ether was added and the deep purple precipitate was collected by filtration and was washed several times with diethyl ether. After two re-crystallisations from MeOH the 84 mg (22.5%) of reddish crystals was collected.

^{1}H-NMR (400 MHz, CD_3CN) δ 7.96 (t, J = 8.6, 1H), 7.06 (d, J = 8.6, 2H), 4.07 (s, 2H), 1.82 – 1.68 (m, 2H), 1.66 – 1.49 (m, 2H), 1.45 – 1.29 (m, 1H), 1.14 (d, J = 6.6, 3H), 1.00 (t, J = 7.4, 3H).

^{13}C-NMR (101 MHz, CD_3CN) δ = 141.02, 138.85, 105.95, 47.56, 33.72, 31.73, 30.19, 19.35, 11.85

MS (MALDI-TOF): m/z: 534 [M$^+$]

ESI-TOF High Resolution Mass Spectrometry: Calculated for $C_{37}H_{48}N_3^+$: m/z = 534.3848; Found: m/z = 534.3871

Synthesis of Oct-DAOTA·BF_4:

Synthesised as described in B. W. Laursen and F. C. Krebs: Synthesis, structure, and properties of azatriangulenium salts *Chem. Eur. J.* **2001,** *7* (8), 1773-1783.

^{1}H NMR (300 MHz, $CDCl_3$) δ = 8.30 (t, *J*=8.7, 1H), 8.10 – 8.01 (m, 2H), 7.45 (d, *J*=8.7, 2H), 7.39 (d, *J*=8.7, 2H), 7.24 (d, *J*=8.1, 2H), 4.55 – 4.41 (m, 4H), 1.91 (s, 4H), 1.59 (d, *J*=9.1, 4H), 1.48 – 1.19 (m, 16H), 0.87 (d, *J*=7.0, 5H).

^{13}C NMR (126 MHz, $cdcl_3$) δ = 152.60, 140.90, 140.57, 139.70, 139.47, 139.06, 111.54, 109.35, 108.94, 107.44, 106.18, 48.35, 31.97, 29.61, 29.38, 26.87, 26.04, 22.83, 14.29.

ESI-TOF High Resolution Mass Spectrometry: Calculated for $C_{35}H_{43}N_2O_4^+$: m/z =507.3375; Found m/z = 507.3389, deviation 2.7 ppm.

Elementary Analysis: Calculated for $C_{35}H_{43}N_2O_4 \cdot BF_4$: C: 70.71, H: 7.29, N: 4.71; Found: C: 70.77, H: 7.32, N: 4.67.

Crystal structure of *N*,*N*’,*N*’’-tris(3-methylpentyl)triazatriangulenium·BF_4

Data were collected on a Nonius KappaCCD diffractometer using Mo Kα radiation and a graphite monochromator. The temperature was kept at 122.4(5) K using an Oxford Cryosystems Cryostream liquid nitrogen cooling device.

Data statistics indicate Laue class -3, and systematic extinctions indicate the spacegroups R3 or R-3. It was not possible based on statistics to determine whether the structure was centrosymmetric. Though data were collected to theta = 27 degrees, it was decided to use the data to a resolution of theta = 23 degrees, as the ratio of signal to background was low, and agreement statics of repeated measurements beyond this resolution became very high.

Solving the structure using traditional direct methods (using the programs SHELXS (1) and SIR(2)) were not successful, however phasing in P1 using the charge-flipping algorithm (3) as implemented in the program superflip (4) resulted in a density that was interpretable. Direct-space symmetry search confirmed the spacegroup R-3 and the structure could be solved and refined in this spacegroup. The structure showed significant disorder in the flexible part of the molecule as well as in the tetrafluoroborate ion, and as a consequence refinement residuals are very high (wR2 = 0.42 , Goof = 2.12) in spite of good internal agreement (R_{int} = 0.033). This prompted us to investigate whether the crystal was merohedrally twinned. Merohedral twin laws were tested in shelxl, however there was no improvement in data refinement residuals, and we conclude that the structure is intrinsically disordered in the flexible alkyl regions and counter ion.

Structure and thermal ellipsoids (50% probability level) of the cation. Hydrogen atoms have been removed for clarity. Only the major fraction of the model of disordered side-chains is shown. Drawing created using the program Mercury (5).

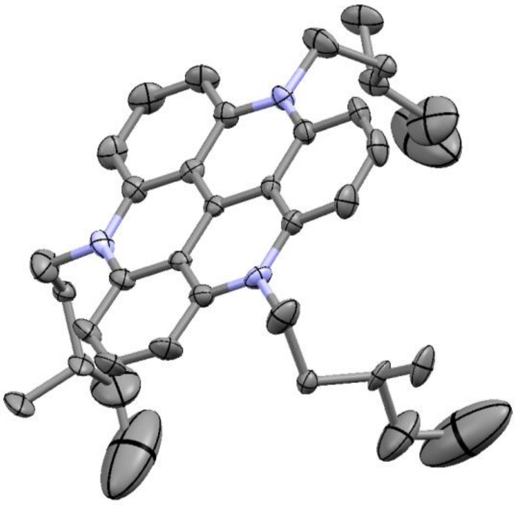

(1) Sheldrick, G.M. (2008). Acta Cryst. A64, 112-122.
(2) Altomare, A.; Burla, M. C.; Camalli, M.; Cascarano, G. L.; Giacovazzo, C.; Guagliardi, A.; Moliterni, A. G. G.; Polidori, G.; Spagna, R. J. Appl. Cryst. 1999, 32, 115-119.
(3) Oszlanyi, G. & Suto, A. (2008). Acta Cryst. A64, 123-134.
(4) Palatinus, L. & Chapuis, G. (2007). J. Appl. Cryst. 40, 786-790.

(5) Macrae, C. F. ; Bruno, I. J. ; Chisholm, J. A. ; Edgington, P. R. ; McCabe, P. ; Pidcock, E.; Rodriguez-Monge, L. ; Taylor, R. ; van de Streek, J. ; Wood, P. A. J. Appl. Cryst., 41, 466-470, 2008.

The table below summarizes the crystallographic data for *N*,*N*’,*N*’’-tris(3-methylpentyl)triazatriangulenium·BF_4:

Crystal Data

Formula	$C_{37}H_{48}N_3^+$, BF_4^-
Formula Weight [g/mol]	207.23
Crystal System	Trigonal
Space group	R-3 (No.148)
a [Å]	12.5700(10)
b [Å]	12.5700(10)
c [Å]	35.496(2)
alpha [Deg]	90
beta [Deg]	90
gamma [Deg]	120
V [$Å^3$]	4857.1(6)
Z	18
D(calc) [g/cm^3]	1.353
Mu(MoKa) [1/mm]	0.090
F(000)	2100
Crystal Size [mm]	0.15 x 0.20 x 0.38

Data Collection

Temperature (K)	122
Radiation [Å]	MoKa 0.71073
Theta Min-Max [Deg]	2.0, 23.2
Dataset	-13: 13 ; -13: 13 ; -39: 39
Tot., Uniq. Data, R(int)	25604, 1549, 0.033
Observed data [I > 2.0 sigma(I)]	1281

Refinement

Nref, Npar	1549, 182
R, wR2, S	0.1209, 0.4275, 2.12
w = 1/[\s^2^(Fo^2^)+(0.2000P)^2^]	where P=(Fo^2^+2Fc^2^)/3
Max. and Av. Shift/Error	0.00, 0.00
Min. and Max. Resd. Dens. [e/Ang^3]	-0.57, 0.76

AFM micrographs of TATA thin films

Tapping mode AFM micrograps of 30 nm thick as cast Octyl-TATA$\cdot$BF$_4$ thin films.

<table>
<tr><td>AFM Micrograph</td><td>Roughness</td></tr>
<tr><td>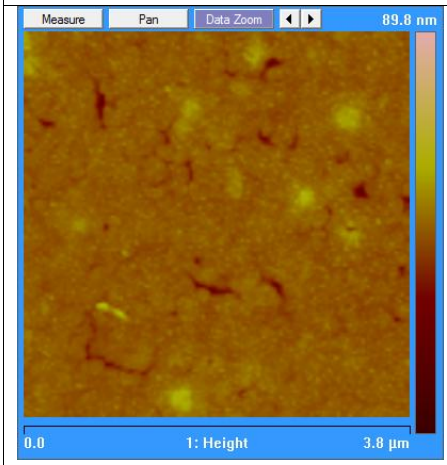
</td><td>13 Å</td></tr>
<tr><td>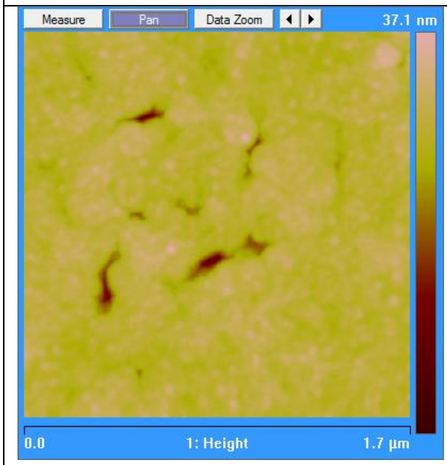
</td><td>10 Å</td></tr>
<tr><td>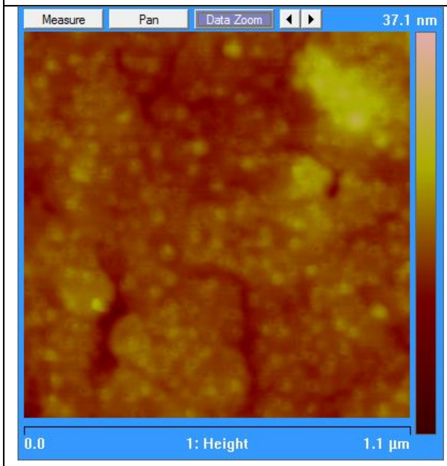
</td><td>19 Å</td></tr>
</table>

Grazing Incidence X-ray Diffraction of TATA$^+$ films

GIXD data for the *N,N'*,*N''*-tris(3-methylpentyl)-TATA•BF$_4$ films

The scattering signal from the thin films was very weak. We tried several collimation setups to achieve the best possible signal to noise ratio. The figure below shows a GIXD pattern acquired under the same conditions as used for the *N,N'*,*N''*-trioctyl-TATA•BF$_4$ films (data shown in paper), i.e. with 0.40x0.40 mm beam at 0.18° incidence angle, which floods the 20x20 mm sample completely.

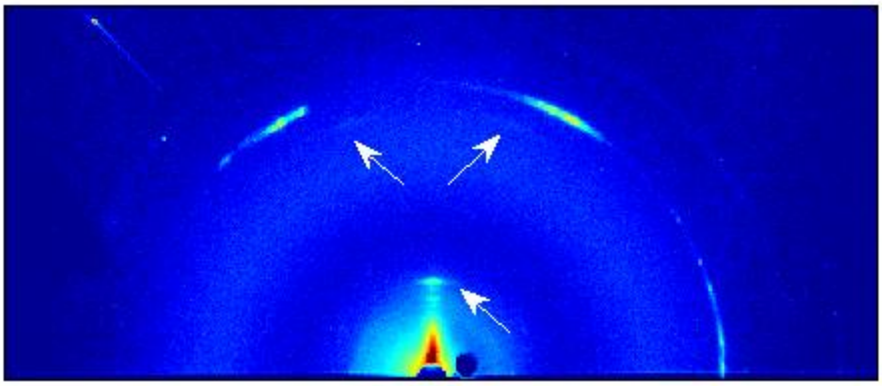

In the figure, we identify three reflections (indicated with white arrows) which are most likely originating from the film, whereas the remaining strong signals are most probably scattering from the silicon substrate.

To improve the signal to noise ratio, we proceeded with a collimation setup, restricting the incident beam to 0.04x0.40 mm, which at 0.18° incidence angle corresponds to a beam footprint of 12.7 mm along the sample surface, smaller than the sample dimension of 20x20 mm. These data are shown below.

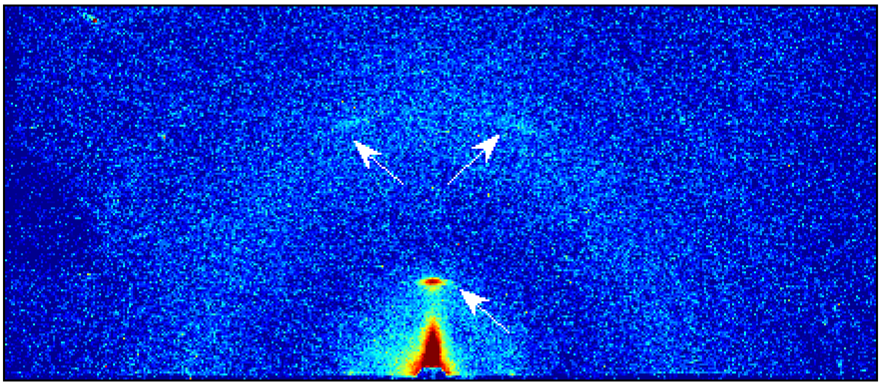

We are able to identify the same three reflections, supporting the assumption that they originate from the film, whereas the remaining scattering features presumably from the substrate are considerably reduced in intensity.

The final data set shows the scattering from an annealed *N,N'*,*N''*-tris(3-methylpentyl)-TATA•BF$_4$ film, acquired with the same narrow beam (0.04x0.40 mm).

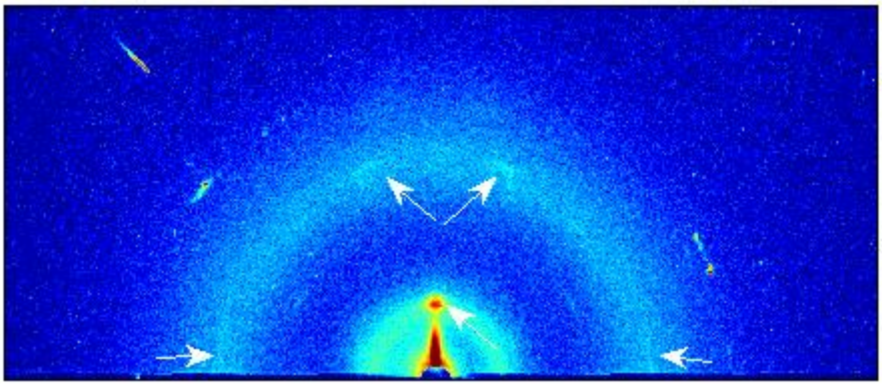

A pair of in plane reflections is seen after annealing, which presumably indicates an improved crystallinity of the films. The three reflections also observed before annealing has moved significantly inwards, corresponding to an expansion of the unit cell. It is difficult to judge whether the weak reflections correspond to the bulk structure of *N*,*N*',*N*''-tris(3-methylpentyl)-TATA•BF_4, simulated in the figure below, although there are distinct similarities.

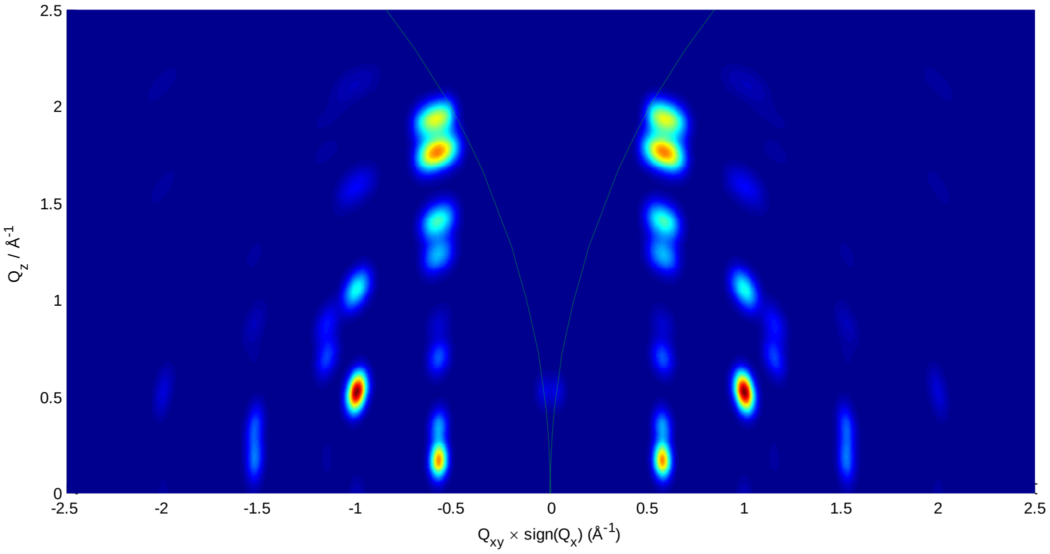

Calculation of Energy Profile

The energy profile for rotating the peripheral alkyl groups in the TATA$^+$ systems are calculated by restricting the angle between the α-β carbon bond and the aromatic plane. This angle is varied in an appropriate range, the structure is allowed to relax and the energy of the system is calculated with DFT (B3LYP/6-31+G(d,p) in SPARTAN®.

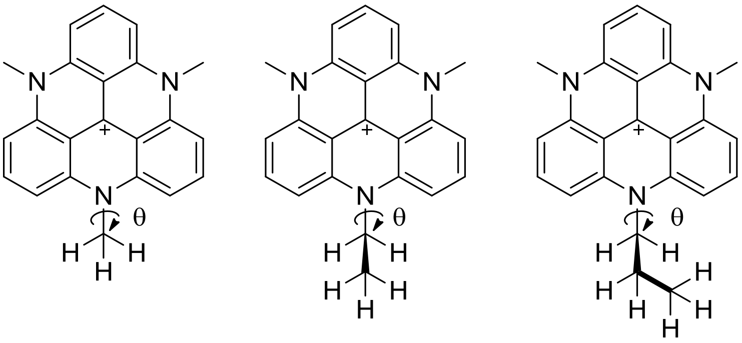

Figure S1. TATA$^+$ compounds used to calculate the barrier for rotation of peripheral alkyl groups.

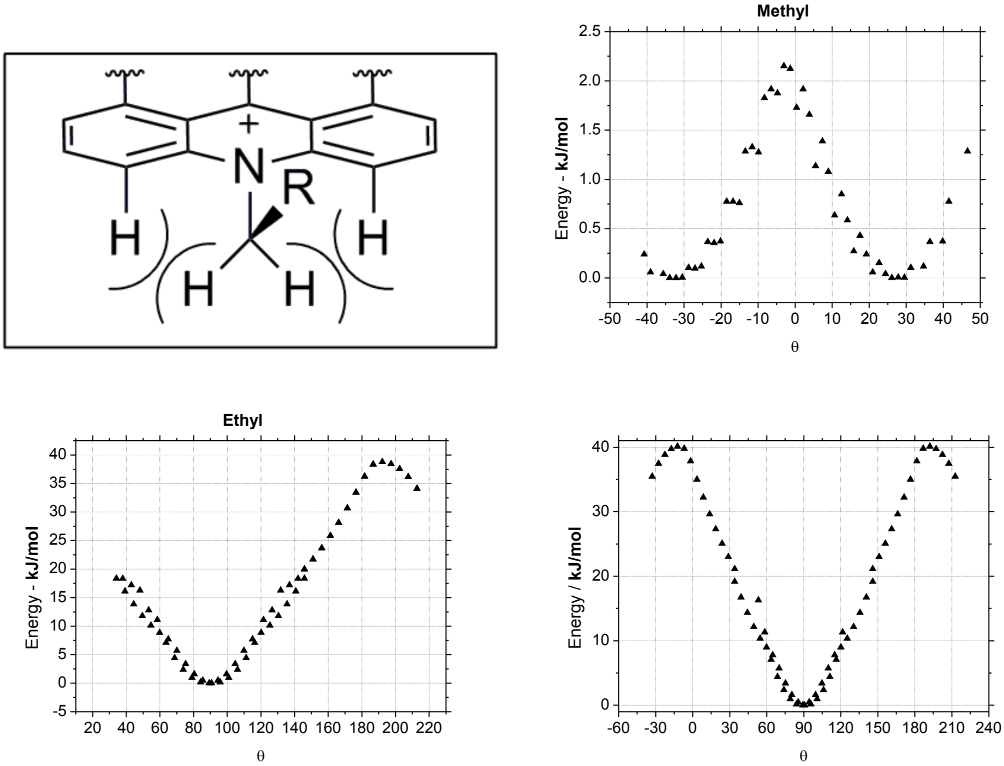

Figure S2. Calculated total energy of *N*,*N*’,*N*’’-trimethyltriazatriangulenium•BF$_4$, *N*,*N*’,*N*’’-ethyldimethyltriazatriangulenium•BF$_4$ and *N*,*N*’,*N*’’-propyldimethyltriazatriangulenium•BF$_4$ as a function of the twist angle θ.

Calculation of Excitation Energies

In order to investigate whether the fluorescence of the energy trap is due to the pure DAOTA dimer or the mixed DAOTA/TATA dimer a series of calculations were done. Since the dimer systems are rather large, density functional theory was the obvious chosen of method for these calculations. The DAOTA and TATA monomers were minimized using Gaussian 03 [1] in vacuum using B3LYP/6- 31+G* with sidechains truncated at methyl which should not influence the electronic properties of the system. The dimers structures were obtained from the crystal structure of Oct -TATA+ , (MePen) -TATA+ and Oct -DAOTA+ , with the alkyl chains truncated at methyl and no counter ions in order to ease the calculation time. All property calculations were done with DALTON 2.0 [2] with the basis set 6-31+G* with the long range corrected functional CAM-B3LYP [3]. All the excitation energies were shifted by +0.7 eV in order to better see the relative connection between the first excited state of the molecular systems compared to the experimental data (See table SX). In order to test the conformation of the DAOTA system several test systems were created by taking two optimized DAOTA molecules and placing them 3.4 Å apart either parallel or anti-parallel. The parallel compound (with the two oxygen atoms above each other) was found to give unrealistic excitation energies and can be disregarded as the structure in the film. The parallel system yielded results almost identical to the crystal structure which indicates that the parallel/crystal structure is the correct one observed in the film. Below, the assigned excitation energies of the first allowed excited state can be seen. In the case of the DAOTA dimer the first excited state is not allowed which is a trend often seen in J-type aggregates which has also been observed in the calculated dimers of ATOTA+ [4].

Compound	λ_{max}(exp)	λ_{max}(calc)	Oscillator Strength
DAOTA monomer	556	551	0.1834
TATA monomer	523	525	0.1403
DAOTA dimer (crystal)	588	587	0.1937
DAOTA dimer (placed 3.4 Å apart)	588	590	0.1776
TATA dimer (Oct Crystal)	548	529	0.1317
TATA dimer (MePen Crystal)	558	535	0.1284
Hetero Dimer	-	591	0.0948

References

[1] Gaussian 03, Revision E.01 Gaussian, Inc., Wallingford CT, 2004.
[2] "dalton, a molecular electronic structure program, Release 2.0 (2005), see http://www.kjemi.uio.no/software/dalton/dalton.html"
[3] Takeshi Yanai, David P. Tew, Nicholas C. Handy, A new hybrid exchange-correlation functional using the Coulomb-attenuating method (CAM-B3LYP), Chemical Physics Letters 2004, 393, 51-57
[4] B.W. Laursen, J. Reynisson, K.V. Mikkelsen, K. Bechgaard and N. Harrit, 2,6,10-Tris(dialkylamino)trioxatriangulenium salts: a new promising fluorophore. Ion-pair formation and aggregation in non-polar solvents, Photochem. Photobiol. Sci. 2005,4 ,568-576

Summary of spectral data for thin films relative to solution spectra

Table S1. The experimental wavelength values for absorption and emission maximum. The shift in maximum is reported for both absorption and emission relative to acetonitrile solution.

Species	Medium	λ_{max} [nm]	λ_{fl} [nm]	Shift abs [nm (cm^{-1})]	Shift fl [nm(cm^{-1})]]
TATA$^+$	solution	523	558	-	-
3-methylpentyl	Thin film[a]	558	599	35 (1200)	41 (1230)
Octyl-	Thin film	548	582	25 (870)	24 (740)
DAOTA$^+$ in solution	solution	559	590	-	-
Octyl DAOTA	Thin film	588	617	29 (880)	27 (740)

[a] Annealed.

Annealing

The effect of annealing was investigated using optical spectroscopy for all involved thin films. The film was placed on a Linkam stage and heating to the indicated temperature for 15 minutes. Afterwards the spectrum was recorded. The method of heating does not correspond to bulk annealing in e.g. a vacuum oven. The temperature of the Linkam stage is not identical to the temperature in the film.

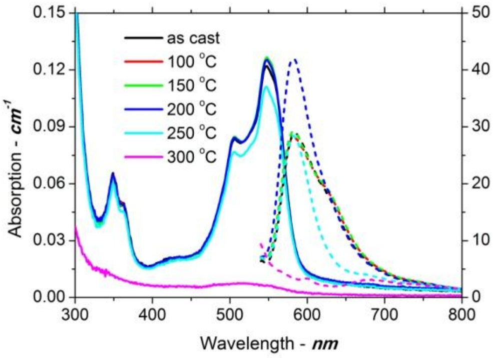

Figure S3. Effect of annealing in *N*,*N*’,*N*’’-tris(3-methylpentyl)-TATA•BF_4 thin films.

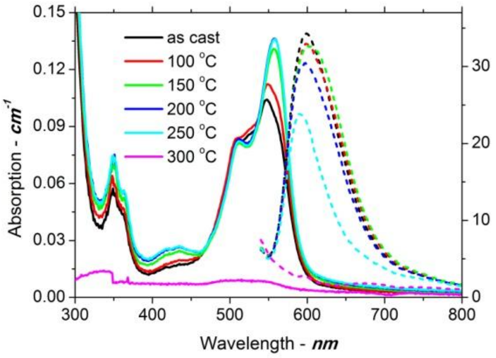

Figure S4. Effect of annealing in *N*,*N*’,*N*’’-trioctyl-TATA•BF_4 thin films.

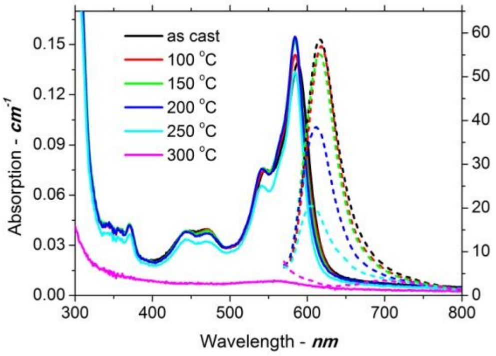

Figure S5. Effect of annealing in *N*,*N*’-dioctyl-DAOTA•BF_4 thin films.

Fluorescence energy transfer from TATA$^+$ to TATA$^+$ and DAOTA$^+$

Förster distance calculations

The Förster distance calculations were performed using the usual formula [38]

$$R_0 = 0.2108\left(\kappa^2 \Phi_D n^{-4} \int I_D(\lambda)\varepsilon_A(\lambda)\lambda^4 d\lambda\right)^{1/6}$$

Where R_0 is the Förster distance in Å, Φ_D is the donor fluorescence quantum yield, $I_D(\lambda)$ the normalized donor fluorescence spectrum ($\int I_D d\lambda = 1$), ε_A the acceptor absorption spectrum, n the refractive index of the medium and κ^2 an orientation factor between 0 (orthogonal transitions) and 4 (colinear transitions).

From the acetonitrile solution spectra (Figure S6) and the measured quantum yield of 0.22 (table 4.1), Förster distances (R_0) of 24 Å and 29 Å can be calculated for the TATA$^+$-TATA$^+$ and TATA$^+$-DAOTA$^+$ donor-acceptor pairs, using 2/3 for the orientation factor κ^2

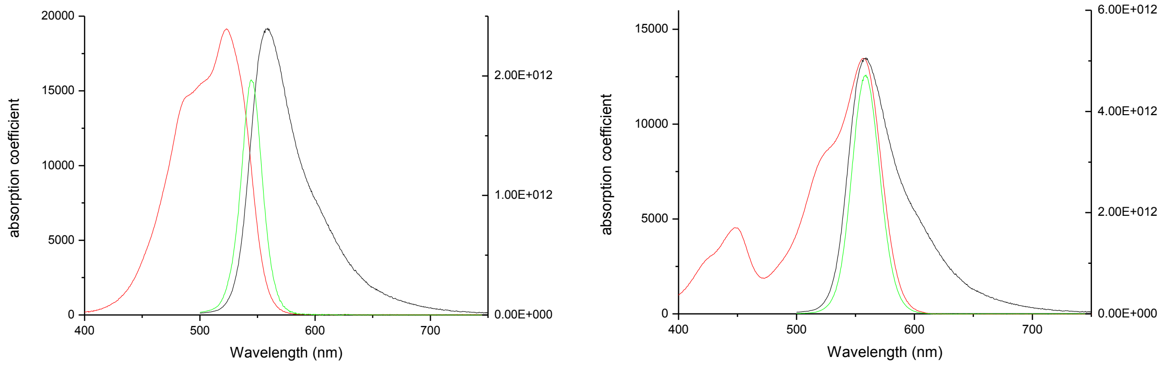

Figure S6. The overlap integral between TATA$^+$ and TATA$^+$ (left) and TATA$^+$ and DAOTA$^+$ (right)

Thin films of *N,N'*-dioctyl-DAOTA•BF

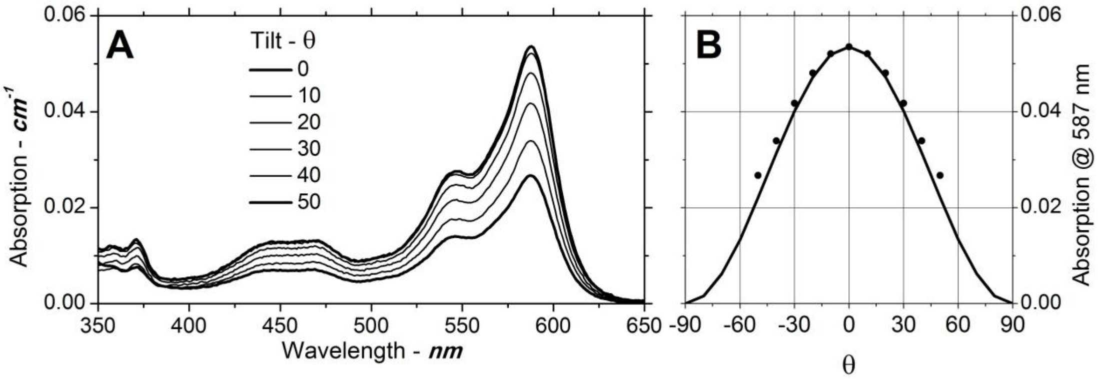

Figure S7. A: Polarized absorption of *N,N'*-dioctyl-DAOTA•BF thin film (5 mg/mL in 1,2-dichloroethane cast at 3000 rpm on glass). Spectra recorded with variable incidence angle (θ). B: Absorption at 587 nm as a function of the angle between incident light and the surface normal. (corrected for change in film thickness by cos(θ)), line correspond to (A@θ=0°) × $\cos^2(\theta)$).

Exciton transport/doping experiments

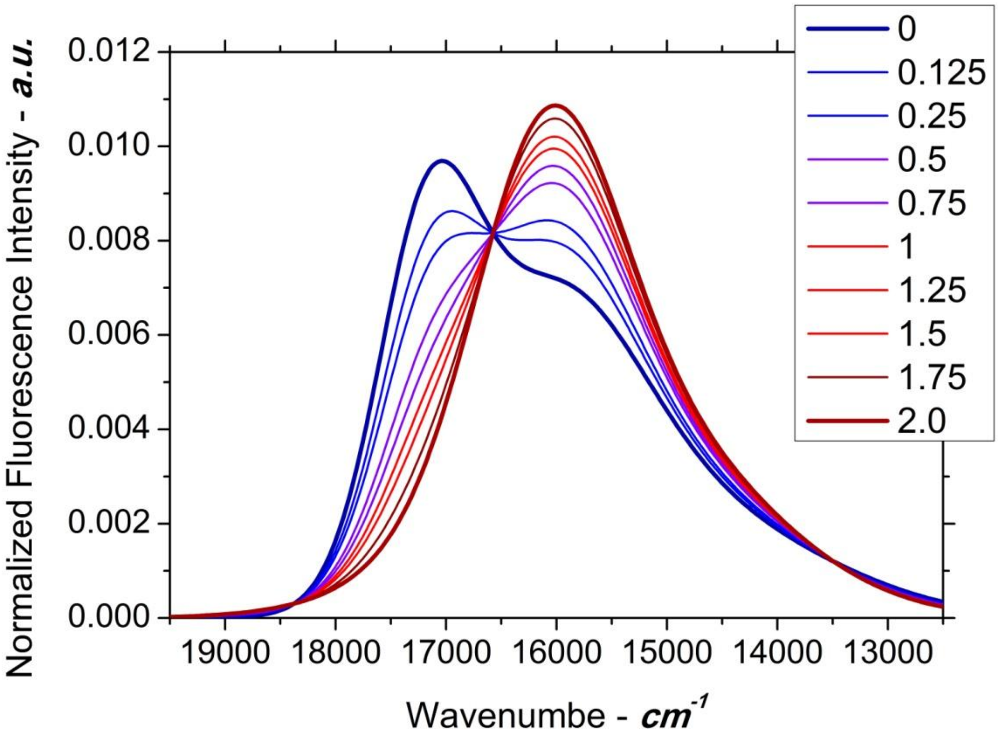

Figure S8. Doping experiment. *N*,*N*',*N*''-trioctyl-TATA•BF_4 films doped with *N*,*N*'-dioctyl-DAOTA•BF_4 in the mol% indicated on the figure.

Table SC. Emission maximum of films with doping mol% 0 and 2.

Doping	λ_{fl}
0 mol%	586
2 mol%	623

Figure S9. Resolved emission spectra of *N*,*N*’,*N*’’-trioctyl-TATA•BF$_4$ films doped with *N*,*N*’-dioctyl-DAOTA•BF$_4$. The spectra are resolved using emission spectra of pure *N*,*N*’,*N*’’-trioctyl-TATA•BF$_4$ and *N*,*N*’-dioctyl-DAOTA•BF$_4$ films.

Doping 0 % - 100 % TATA

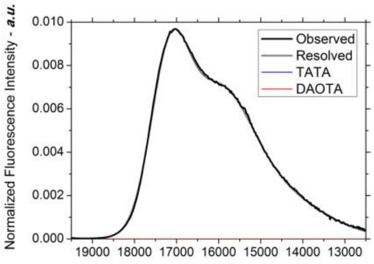

Doping 0.125 % - 79 % TATA

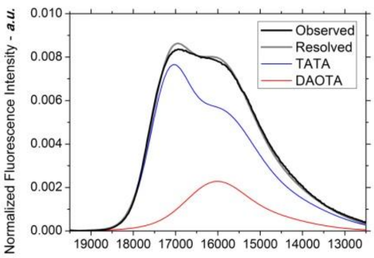

Doping 0.25 % - 67 % TATA

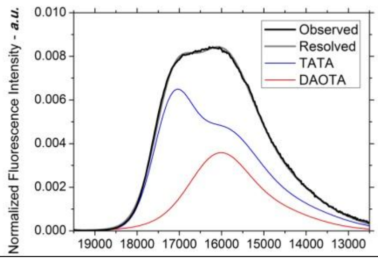

Doping 0.5 % - 45 % TATA

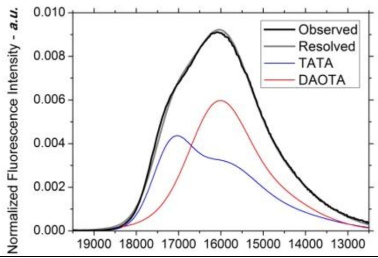

Doping 0.75 % - 35 % TATA

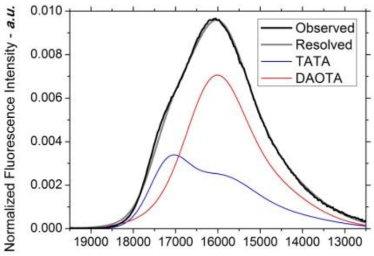

Doping 1.0 % - 25 % TATA

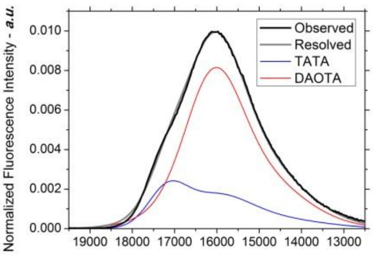

Doping 1.25 % - 18 % TATA

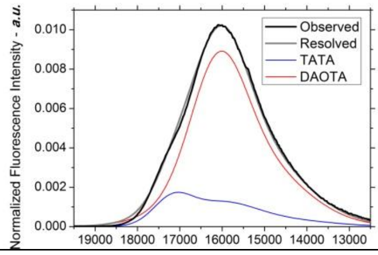

Doping 1.5 % - 7.5 % TATA

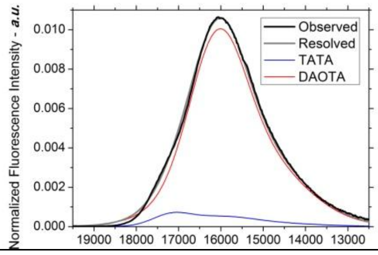

Doping 1.75 % - 7.5 % TATA

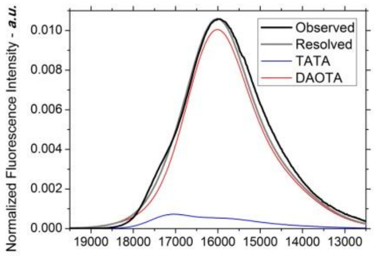

Doping 2.0 % - 100 % DAOTA